**Article:**
Thornley, B, Beadling, R, Bryant, M et al. (1 more author) (2020) Investigation of the Repassivation Process of CoCrMo in Simulated Biological Fluids. CORROSION, 76 (6). pp. 539-552. ISSN 0010-9312

https://doi.org/10.5006/3423

# Investigation of the Repassivation Process of CoCrMo in Simulated Biological Fluids

*Blake Thornley,*, *** Robert Beadling,* Michael Bryant*, and Anne Neville**

Faculty of Mechanical engineering, University of Leeds, LS2 9JT

Article history

Received Day Month Year
Accepted Day Month Year
Available Day Month Year

Keywords:

A. CoCrMo Alloy
B. Repassivation
C. Bio-Material
D. Corrosion

* University of Leeds, Leeds, LS2 9JT.

***Corresponding author: Blake Thornley, Email: cm12bjt@leeds.ac.uk

## ABSTRACT

A thorough investigation into the repassivation process of CoCrMo in multiple simulated biological environments has been undertaken, looking in detail at both the kinetics and composition of the reformed oxide film. Specific focus of this research was aimed at determining the effect of bovine serum albumin (BSA) on these features. The kinetics of repassivation were obtained by using a variety of electrochemical techniques, the current transients formed were fitted to a second order decay curve which accouts for two separate phases: coverage and growth. The reformation of the passive film was fastest in a PBS environment, with the presence of BSA delaying this process as it inhibits the oxygen reduction reaction as it obstructs the active sites of the alloy when adsorbed onto the surface. The composition of the newly formed film was analysed with X-Ray photoelectron spectroscopy (XPS). As expected the film was primarily composed of chromium (III) oxide with small contributions from cobalt and molybdenum oxides. In the presence of BSA the quantity of molybdenum within the film was drastically reduced, via use of Inductively Coupled Mass Spectroscopy (ICP-MS) it was shown to be extracted into the bulk solution. This observation is due to BSA being able to complex preferentially to the molybdenum ions when the alloy is exposed, extracting them into solution altering the composition and integrity of the film.

## INTRODUCTION

Orthopaedic surgery has become one of the most common and successful treatments for people suffering from issues involving their musculoskeletal system[1]. In cases of arthritis and rheumatism around the weigh-bearing joints, hip and knee, prosthetic joint replacement is often needed to ease suffering and restore mobility. This process has advanced massively over the last 50 years due great investment in terms research and clinical trials, which has been vital as the need for joint replacement among the population has drastically increased over the years. According to statistics around 350,000 primary hip replacements were undertaken in the USA alone, with this number expected to rise to 500,000 a year by 2020.[2]

Metal on metal (MoM) hip joints have been used since the early 1990's, due to adverse effects in the previously used metal on polymer (MoP) joints in which wear particles induced osteolysis.[1,3,4] CoCrMo alloys were one of the MoM joints developed as the alloy possesses excellent biocompatibility, low wear rates and a high corrosion resistance as an oxide film is spontaneously formed on the surface which acts as a barrier to the environment. The main constituent of the passive film is chromium (III) oxide with some minor contributions of cobalt (II) oxide and molybdenum oxides (IV-VI). A vital attribute of this alloy is its high postulated longevity which is essential seeing as there is a greater demand for a replacement among the younger population.[4] Some MoM devices have lasted for up to 25 years in-vivo with recorded wear rates lower than that of MoP joint.[1] Over the last few years, issues have arisen with MoM devices, as over time metal ions are released into the body and if they are absorbed by erythrocytes it can lead to genotoxicity within the patient.[5] This finding makes the need to identify the origin and quantify of metal ion released when discussing the safety of these devices.

The physiological environment has an effect on the electrochemical behavior of the implanted alloy. The alloy is exposed to synovial fluid in the body, which is a viscous, non-Newtonian fluid present in the cavity to help reduce friction during motion. This fluid is mainly comprised of Human Serum Albumin, a small globular protein containing 585 amino acid chains linked together by 17 disulfide bonds.[6,7] Due to its high concentration and mobility within the fluid it determines the majority of the surface/environment interactions as it arrives first at the implant.[7] For experimental purposes, Bovine Serum Albumin is used to mimic a biological environment as it's a model of Human Serum Albumin.

The effects of BSA on the corrosion resistance of CoCrMo has been studied by Yan et al,[8] he observed that the presence of BSA can be two fold. It can accelerate metal dissolution via binding to the metal species but was shown to also act as a lubricant reducing friction and therefore mass loss. Espallargas et al,[9] noted an increase in molybdenum ions released into solution in the presence of BSA under electrochemical conditions for a range of different domains. Although the electrochemical behavior of CoCrMo alloys has been investigated to a great extent in recent years, there has not been a comprehensive study into the repassivation kinetics of the alloy. Repassivation is the process in which when the passive film has been compromised/removed it re-establishes itself via oxidation of the metal surface. This is vital in evaluating the corrosion resistance of the metal as the higher the rate of repassivaiton the less corrosion takes place when the alloy is exposed. Williams et al,[10] carried out some in-vitro wear tests on a range of alloys and concluded that the presence of protein can alter the repassivated oxide layer as well as form metal-chloride complexes.

The focus of this paper is to fully determine the interactions of the surface/environment of CoCrMo alloys exposed to a protein-containing environment during electrochemical repassivation and its subsequent effect on the composition of the resulting oxide film formed, which has been missing from the literature. A range of electrochemical techniques have applied to measure corrosion rates with post-test assessment to assess the mechanisms that have taken place. Surface characterization was employed to analyze changes in the surface once repassivation had

occured and compared to a passivated layer to determine the effect of the environment on the process. Inductively coupled plasma mass spectroscopy (ICP-MS) was conducted to determine the quantity of metal ions released throughout a single repassivation phase.

## THEORY OF REPASSIVATION

Once the oxide layer has been stripped from the CoCrMo alloy, the metal will be exposed to the environment. The metal elements are either oxidized and lost to the solution or react with the oxidants to reform the passive film, the preference of these reactions can be manipulated via electrochemical means. Both of these processes produce free electrons, which are detected as current transients. Both the general dissolution and passivation pathways for the metal ions are depicted in Equation 1.

$$M_{(s)} \rightarrow M_{(aq)}^{n+} + ne^-$$

$$M_{(s)} + O_{2_{(g)}} \rightarrow MO_{2_{(S)}}$$

$$M_{(s)} + \frac{n}{2}H_2O_{(l)} \rightarrow MO_{n/2_{(s)}} + nH_{(aq)}^{+} + ne^-$$

**EQUATION 1:** *Shows the general dissolution and passivation pathways for metal ions*

The current transient formed is the sum of dissolution and oxide film growth currents from the exposed alloy, several models have been proposed over time to interpret this. The model put forward from Ambrose [11] stated that as the oxide film is forming, the area fraction covered by oxide ($\theta$) increases as time does. If film thickness is assumed to be constant then the current related with the growth is as follows:

$$i_{film} = \frac{nF\rho v}{M_w}\frac{d\theta}{dt}$$

**EQUATION 2:** *The equation for the current formed from oxide film growth[11,12]*

Under these kinetics, the rate of film growth, $i_{film}$ depends on Faradays Law and the rate of regrowth of the oxide film. $\rho$ is the density of the film, $V$ is the total volume of oxide to grow, $M_w$ is the molecular weight of the film and $n$ is the total charge transferred.

For ionic dissolution, if Tafel-like behavior for the bare metal is assumed then the current formed can be expressed as:

$$i_{diss} = i_0^{diss}(1-\theta)e^{\frac{V-V^{eq}}{\beta}}$$

**EQUATION 3:** *The equation for the current formed by ionic dissolution[11,12]*

Where $i_0^{diss}$ is the dissolution exchange current density across the bare metal, $V$ is the voltage away from the equilibrium potential for the bare metal dissolution reaction and β is the Tafel constant for the reaction. This differential equation results in an exponential time decay of the total current when the surface is held at a fixed potential. While there are many assumptions associated with this model, it gives a good interpretation of the process and had been used to explore responses in the removal of oxide.[11]

Therefore the total anodic current produced from these equations is indicated by:

$$i = i_{film} + i_{diss} = \frac{nF\rho v}{M_w}\frac{d\theta}{dt} + i_0^{diss}(1-\theta)e^{\frac{V-V^{eq}}{\beta}}$$

$$\text{Where} \quad \theta(t) = 1 - e^{(\frac{-t}{\tau})}$$

**EQUATION 4:** *The equation for the total anodic current produced[11,12]*

This differential equation results in an exponential time decay for the total current. Goldberg et al,[13] were the first to note this and proposed fitting the current transient to a first order exponential decay curve to determine the kinetics of repassivation in various electrolytes during tribo-corrosion. This model was then developed by Sun,[14] who found that a second order decay curve gives a better fit to the current transient. The second order reflects the complexity of the reforming of the oxide which is dependent on the rate of oxygen diffusion to the surface. The equation for this can be seen below:

$$I(t) = I_1 e^{(\frac{-t}{\tau_1})} + I_2 e^{(\frac{-t}{\tau_2})} + I_3$$

**EQUATION 5:** *The second order decay fit[14,15]*

Where I(t) is the total current formed with respect to time, t is the time taken, $I_1$ and $I_2$ are the maximum currents of the exponential curves produced, $\tau_1$ and $\tau_2$ are the time constants of the respective exponential decay curves with $I_3$ being the steady state current achieved as the time constants diminish. By applying this we are enabled to account for both the oxide coverage and thickening phases that occurs during repassivation.

The integrity of the film formed on the surface of the metal can also be determined from the current transients by plotting them on a Log-Log scale which allows the repassivation index to be obtained via analysis of the slope.[15] The empirical form and Log-Log equation is seen in Equation 6 below. When n = 1, the passive film is highly ordered and compact with the porosity increasing as the slope approaches closer to zero.[15] These values were obtained from analysis of $\tau_2$ as that's when the film was fully formed.

$$i(t) = At^{-n}$$

$$Log(i) = Log(A) - nLog(t)$$

**EQUATION 6:** *The Log-Log Equation to determine the repassiavtion index[15,17]*

# MATERIALS AND METHODOLOGY

## *Metal and Solutions under Investigation*

LC CoCrMo (ASTM 1537-94) was the alloy investigated, plates of a thickness of 3 mm with Ø = 6 mm were cut from rods. Table 1 below shows the composition of the alloy used, which is relative to ASTM standards. [18]

| | Co % | Cr % | Ni % | Mo % | C % | Other |
|---|---|---|---|---|---|---|
| **CoCrMo** | 66 | 27 | 0.2 | 5.5 | 0.04 | - |

**TABLE 1:** *The composition of LC CoCrMo (ASTM 1537-94)*

The environments that the corrosion behavior of CoCrMo were analysed in were saline (0.9%) and phosphate buffered saline (PBS), with differing quantities of bovine serum albumin (BSA, 96%, Fischer Scientific) present ranging from 0 to 4g/L. Table 2 indicates the composition of PBS solution. The saline solution represents simple simulated bodily fluids as its level of chloride ions is comparable to that of a human, the effect of phosphates was analysed by use of PBS solution. BSA was used to mimic a more realistic environment, as it is a model protein of human serum albumin (HSA) and to observe the effects of protein and its concentration on the corrosion resistance and the mechanisms that occur.

| Compound | Concentration (mmol/l) | Concentration (g/l) |
|---|---|---|
| NaCl | 137 | 8.00 |
| KCl | 2.70 | 0.20 |
| $Na_2HPO_4$ | 10.0 | 1.44 |
| $KH_2PO_4$ | 1.80 | 0.24 |

**TABLE 2:** *Indicates the individual components of PBS solution*

## *Sample Preperation*

The metal sample was mechanically polished using a Buehler Grinder Polisher to achieve a target surface roughness of ~10nm. This was achieved by first wet grinding the sample with SiC paper of a roughness of 120 followed by 320, 600, 800 and 1200. Polishing of the sample was then undertaken by using diamond suspension of 6 micron then 3 micron giving a mirror like finish. The sample was then cleaned with deionised water and dried by using compressed air before the experiment was carried out

## *Electrochemical Setup*

A custom designed sample holder was made to hold the polished sample, shown in figure 1. This meant that after the electrochemical tests were undertaken the sample could easily be withdrawn and undergo surface analysis. The sample is connected to the potentiostat as is sits on a copper plate within the holder welded to a wire that can easily be connected, an area of 0.13cm$^2$ was exposed to the environment. A good contact to the copper plate is ensured due to the removable lid which is held tightly with screws.

.

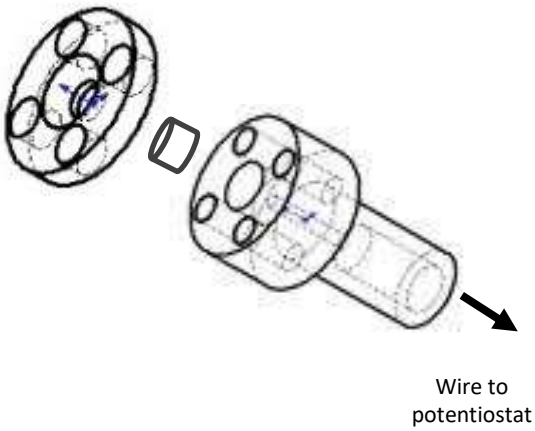


**FIGURE 1:** *The designed sample holder used for the electrochemical tests (Acts as WE)*

The electrochemical behavior was analysed by use of a potentiostat (Princeton Applied Research potentiostat/galvanostat Model 263A) which was controlled via a computer. A three electrode cell was utilized which consists of the working electrode (WE) shown in figure 1, a reference electrode (RE) which was Ag-AgCl as it possesses a well-defined potential and a platinum counter electrode (CE).

Open circuit potential (OCP) was monitored for 1 hour to allow for stabilization before the tests were conducted, this was conducted at a rate of 1 point per second.

The overall corrosion behavior of the alloy was evaluated by undertaking both anodic and cathodic polarization curves in the various electrolytes, these tests were undertaken right after OCP was achieved. The potentiodynamic polarization scan rate was 0.25 mV/s either being ramped up to $1V_{RE}$ for the anodic tests and down to $-1V_{RE}$ for the cathodic ones. Tafel analysis was undertaken to analyze the polarization graphs obtained by extrapolating the linear portions of the graph to the point at which they intersect, the process is shown below in Figure 2. Separate tests were carried out for the two regions to avoid drastic changes across the surface by doing a complete scan which could affect the electrochemical behavior.

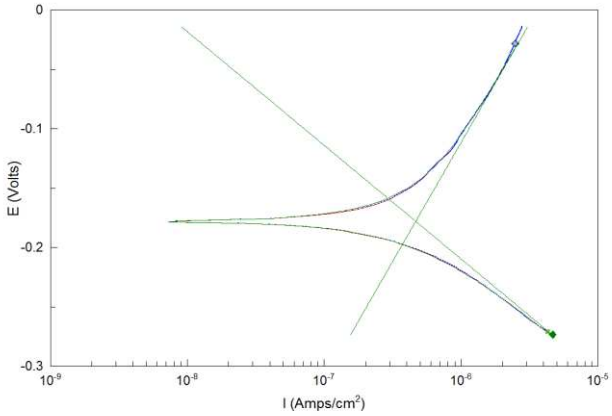


**FIGURE 2:** *Example of Tafel exptrapolation process for CoCrMo in PBS solution*

For the investigation of repassivation kinetics the samples were polarized at -1 $V_{RE}$ for 30 minutes to strip the oxide film before being shifted to a passive potential of +0.1 $V_{RE}$ for another 30 minutes to induce repassivation. The rate the resultant currents were sampled at was 100 Hz. These specific potentials were defined from the potentiodynamic experiments (anodic and cathodic) carried out previously. The passive potential was chosen as it is well within the passive domain for all conditions, whereas the cathodic potential was chosen as its more negative than that of the standard electrode reduction potential of $Cr/Cr^{2+}$ yet more noble enough not to incur the evolution of hydrogen. This is also concurrent with the pourbaix diagram of Cr.[19]

Before these kinetics were investigated, impedance (EIS) was undertaken to determine the electrochemical differences in the properties of the interface of the alloy at these specific passive and cathodic conditions. These EIS experiments were conducted by use of the Multi Autolab M204 utilizing the FRA32M module.The samples were polarized at their respective potentials chosen for 10 frequency decades from 1mHz to $10^5$ Hz at an amplitude of ± 10mV. The obtained data was the scrutinized by use of Nova 2.1 and fitted to its equivalent circuit. An example of the electrochemical circuit fit is shown in Figure 3, all fits were obtained with suitable $X^2$ values ($10^{-4}$) with each component possessing an error of less than 5%.

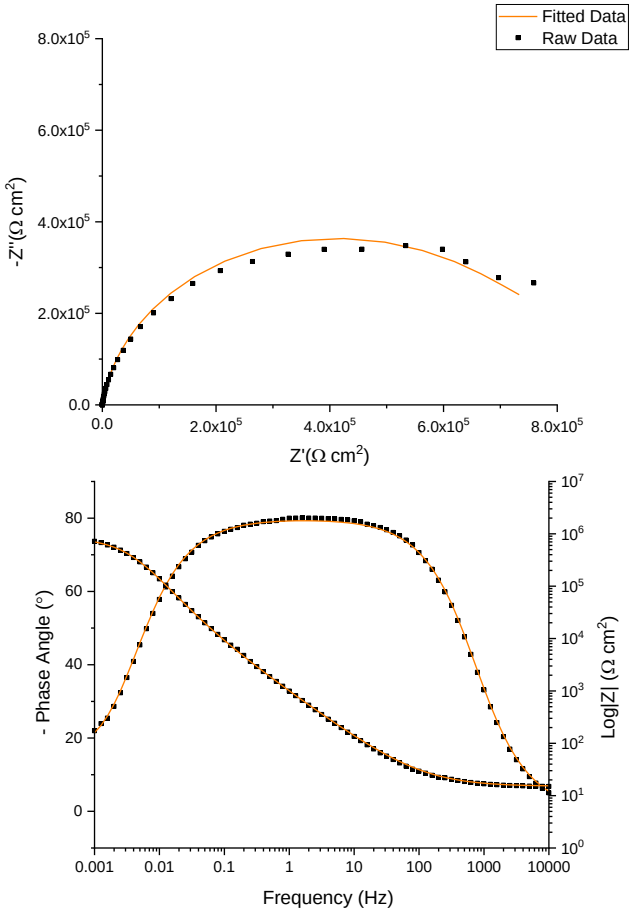


**FIGURE 3:** *Example of Fitted cell to the passive impedance spectra of CoCrMo in a PBS environment*

## *Surface Characterisation*

XPS measurements were conducted using a monochromated aluminium K-alpha X-Ray source with the Thermo Escalab 250. To ensure no movement of the sample occurred they were mounted using carbon tape to the stage. The power was set to 150W with the size of the sample area being 500µm. Specific individual peaks were analysed in detail at a step size of 0.1eV with an energy of 20eV, optimizing the number of scans for each to ensure a good signal/noise ratio. By setting the carbon 1s peak to 285eV and applying this it to all spectras of the set the binding energy could be calibrated. Depending on the baseline of the individual peaks either a linear or Shirley baseline fit was used with the peaks then being fitted and deconvoluted in accordance with the literature.[20]

## *Metal Ion Concentration*

The concentration of metal ions released to the solution was measured after the repassivation experiments had been conducted using the Elan DRce (Perkin Elmer). The solutions of the three repetitions of each tests were analyzed, before analysis the samples were stabilized by making up to 2% $HNO_3$ with any particulate matter being filtered off by use of a centrifuge. The isotopes of metal ions under analysis were Co 59, Cr 52 and Mo 98.

# RESULTS

## *Corrosion Behavior*

Figure 4 shows the obtained OCP data in various electrolytes with the final values being shown in Table 3. From the figure it is seen that the OCP values tend to increase to more noble values over the course of time. From the different steady state values achieved it shows that the solution chemistry plays a vital role. The presence of phosphates increase the value of OCP indicating they act as an anodic inhibitor while the BSA acts as a cathodic inhibitor by reducing the values. The more BSA is added the greater the effect of cathodic inhibition and therefore a lower value of OCP occurs.

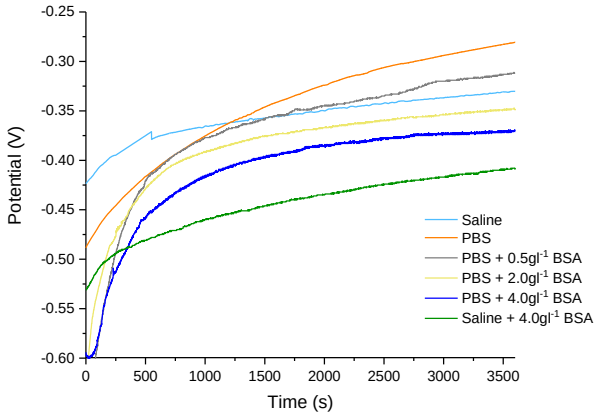


**FIGURE 4:** *The OCP curves for CoCrMo in simulated bodily fluids over an hour*

Both the anodic and cathodic polarization curves for CoCrMo in the various electrolytes are shown in Figure 5 with the extracted values from each graph being shown in Table 3.

The anodic curves are shown in Figure 5a, the anodic domain is at potentials higher than that of the $E_{corr}$ where a transition from cathodic to anodic current occurs. A current density increase is seen above $E_{corr}$ as the metal alloy is active resulting in corrosion taking place. Passivation of the sample is indicated when the current density stabilizes due to formation of the oxide film which protects the surface from the environment, it is seen that phosphates decrease the passive current density while BSA increases it. When the potential is shifted high enough trans-passive behavior occurs which causes the film to breakdown resulting in corrosion to occurring once more. The phosphates are seen to activate transpassive dissolution due to the formation of phosphate chromium complexes which activate dissolution indicated by the dissolution occurring at lower values than that of just a saline solution.

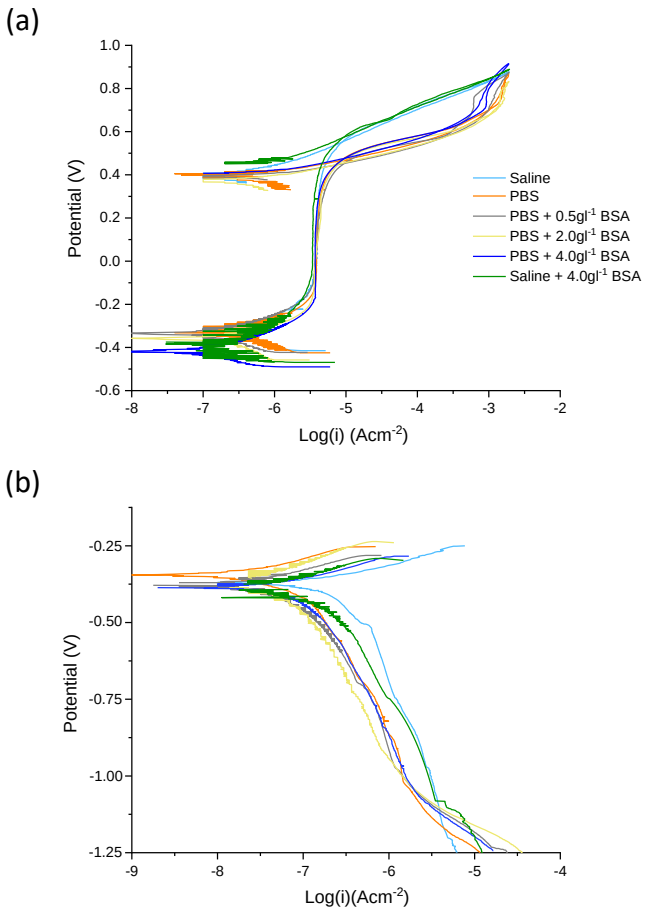


**FIGURE 5:** *The Anodic (a) and Cathodic (b) potentiodynamic curves for CoCrMo in simulated bodily fluids*

| Electrolyte | OCP/$E_{corr}$ (V) | $I_{corr}$ (µA/cm²) | $I_{pass}$ (µA/cm²) | $E_b$(V) | $E_r$ (V) |
|---|---|---|---|---|---|
| Saline | -0.33 ± 0.02 | 0.18 ± 0.05 | 3.82 ± 0.04 | 0.52 ± 0.02 | 0.56 ± 0.03 |
| PBS | -0.28 ± 0.01 | 0.12 ± 0.04 | 3.42 ± 0.06 | 0.46 ± 0.04 | 0.47 ± 0.02 |
| PBS + 0.5gl$^{-1}$ BSA | -0.31 ± 0.02 | 0.24 ± 0.03 | 3.53 ± 0.05 | 0.45 ± 0.01 | 0.46 ± 0.03 |
| PBS + 2.0gl$^{-1}$ BSA | -0.36 ± 0.04 | 0.28 ± 0.03 | 3.59 ± 0.07 | 0.48 ± 0.03 | 0.47 ± 0.01 |
| PBS + 4.0gl$^{-1}$ BSA | -0.39 ± 0.02 | 0.29 ± 0.02 | 3.74 ± 0.03 | 0.46 ± 0.03 | 0.48 ± 0.02 |
| Saline + 4.0gl$^{-1}$ BSA | -0.43 ± 0.02 | 0.39 ± 0.04 | 3.91 ± 0.06 | 0.54 ± 0.03 | 0.58 ± 0.02 |

**TABLE 3:** *The extracted values obtained from the electrochemical experiments undertaken*

The cathodic curves for CoCrMo in the various electrolytes are shown in Figure 5b, the cathodic domain is at potentials lower than the $E_{corr}$ where the current is determined by the reduction of oxygen and the reduction of other species when there is a sufficient thermodynamic driving force. Initially after $E_{corr}$ there is an increase in current density due to oxygen being reduced, this is limited by how fast the molecules can move into solution. The presence of both phosphates and BSA hinder this movement indicated by diminished currents. The current then remains fairly stable until around -1.10V where reduction of phosphate/BSA species occurs, there is no further reduction of species seen in just a saline environment.

The EIS for the passive potential of +0.1$V_{RE}$ is shown in Figure 6 with the fitted electrical circuit being displayed in Figure 7 and its respected extracted values for each electrolyte in Table 4.

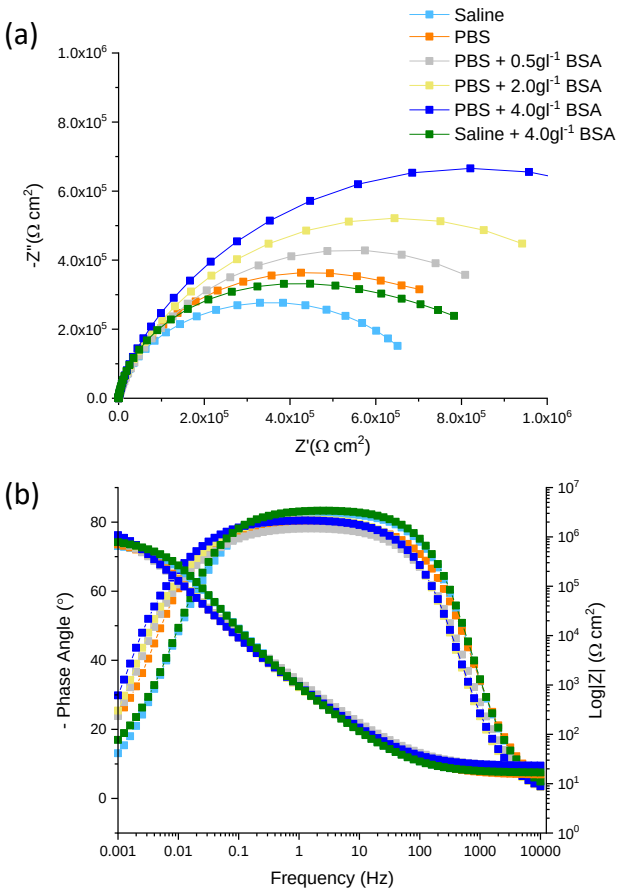


**FIGURE 6:** *Shows the Nyquist (a) and bode plots (b) of CoCrMo under passive conditions in simulated bodily fluids*

The plots shown display typical passive behavior characterised via high impedance values whilst also exhibiting capacitive behavior which is indicated via the semicircle shape obtained. As there are two points of inflection within the bode plot it implies that the cell consists of two time constants.
One of these time constants corresponds to the oxide resistance ($R_{in}/C_{in}$) with the second being attributed to charge transfer resistance ($R_{out}/C_{out}$). A constant phase element is then introduced instead of the capacitor as it accounts for the non-ideal behavior of the capacitive elements due to the various physical phenomena such
as surface heterogeneity which is a result from surface roughness, impurities, dislocations and the presence of grain boundaries.

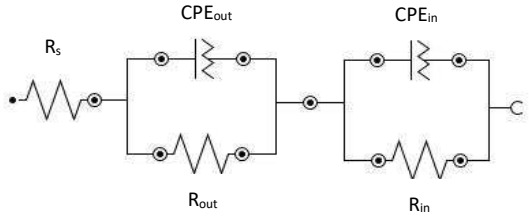


**FIGURE 7:** *Equivalent circuit used to analyse the impedance spectra obtained under passive conditions. $R_s$ solution resistance, $R_{out}$ outer layer resistance, $CPE_{out}$ CPE of the outer layer, $R_{in}$ inner layer resistance, $CPE_{in}$ CPE of the inner layer*

From the extracted data, it is clear to see that the environment in which passivation occurs has a drastic effect on the properties of the alloy. In a phosphate containing environment, the resistance is drastically increased with the values of $R_{out}$ and $R_{in}$ almost doubling compared to just a saline condition. As well as improving the corrosion resistance the thickness of the passive film increases due to a lower value of $CPE_{in}$.
The influence of BSA caused different features on the spectrum obtained, shifting the phase angle towards lower frequencies. It is also seen to increase values of $R_{out}$ and $R_{in}$, although in the presence of phosphates the effect on $R_{in}$ is minimal. The value of $CPE_{out}$ decreases indicating that albumin is deposited on the surface, the higher the concentration the thicker the layer is.

| Electrolyte | $R_s$ ($\Omega$ cm$^2$) | $R_{out}$ (M$\Omega$ cm$^2$) | $CPE_{out}$ ($\mu$F/cm$^2$) | $n_{out}$ | $CPE_{in}$ ($\mu$F/cm$^2$) | $n_{in}$ | $R_{in}$ (M$\Omega$ cm$^2$) |
|---|---|---|---|---|---|---|---|
| Saline | 13.4 | 0.42 | 1.90 | 0.90 | 2.29 | 0.85 | 0.26 |
| PBS | 15.3 | 0.76 | 1.02 | 0.92 | 1.75 | 0.88 | 0.46 |
| PBS + 0.5gl$^{-1}$ BSA | 22.4 | 0.84 | 0.88 | 0.91 | 1.97 | 0.88 | 0.49 |
| PBS + 2.0gl$^{-1}$ BSA | 22.6 | 0.98 | 0.75 | 0.93 | 2.05 | 0.88 | 0.46 |
| PBS + 4.0gl$^{-1}$ BSA | 23.0 | 1.15 | 0.72 | 0.92 | 2.13 | 0.88 | 0.48 |
| Saline + 4.0gl$^{-1}$ BSA | 16.7 | 0.64 | 1.55 | 0.93 | 2.90 | 0.87 | 0.42 |

**TABLE 4:** *The extracted values obtained from the electrochemical fitted circuit for passive conditions*

The Impedance spectra for the cathodic potential of -1.0$V_{RE}$ is shown in Figure 8 with the fitted electrical circuit being displayed in Figure 9 with its respected extracted values for each electrolyte in Table 5.

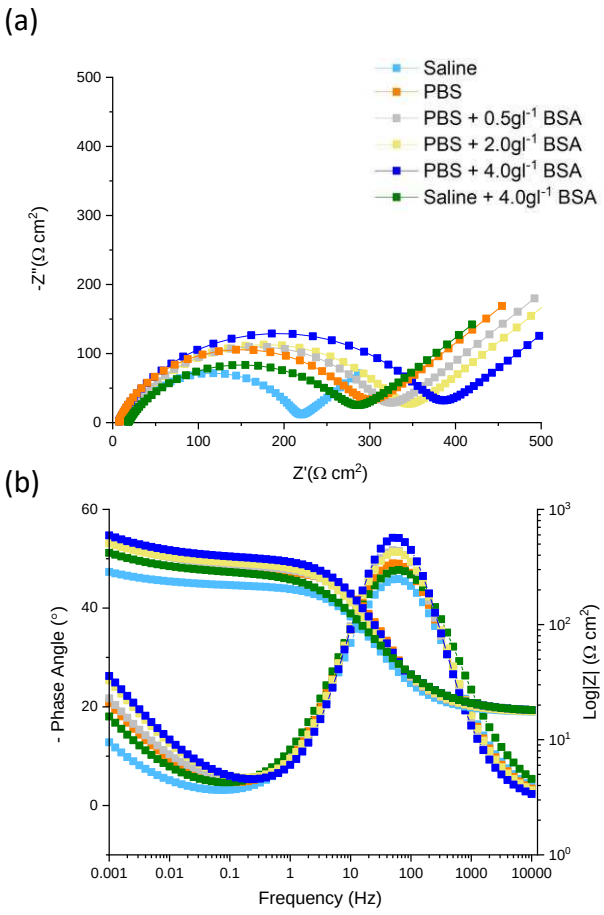


**FIGURE 8:** *Shows the Nyquist (a) and bode plots (b) of CoCrMo under passive conditions in simulated bodily fluids*

The Nyquist plots are composed of a small semi-circle at high frequency followed by a line at low frequency, which indicates the presence of a diffusion controlled reaction this is characterized via warburg impedance.

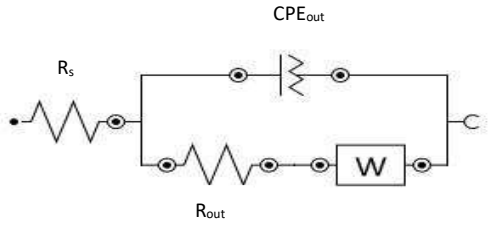


**FIGURE 9:** *Equivalent circuit used to analyse the impedance spectra obtained under passive conditions. $R_s$ solution resistance, $R_{out}$ outer layer resistance, $CPE_{out}$ CPE of the outer layer, W Warburg diffusion*

In the presence of phosphates the values of $R_{out}$ increases alongside a lower value of $CPE_{out}$ indicating that there is an increase in thickness to the interface and corrosion resistance, further supporting the theory that phosphates adsorb onto the surface on the alloy. This presence of an adsorbed film also leads the value of diffusion to decrease. When albumin is present in the environment the quantity of $R_{out}$ increases with $CPE_{out}$ decreasing even further indicating that the molecules are absorbed on the surface. Due to the size of the molecules, the level of diffusion is further reduced. The more BSA is present the stronger these effects become.

## *Repassivation Kinetics*

The re-passivation behavior of CoCrMo has been investigated by the use of current transient curves where the metal was cleaved of the oxide film by cathodic protection as described in the experimental section. Figure 10 shows the data obtained when the potential was shifted to the passive potential, upon initial passivation the current is seen to increase as corrosion of the metal is occurring on the surface due to anodic oxidation giving off metal ions and electrons before slowly decreasing due to formation of the passive film. It is seen that the rate of repassivation is greatly affected by the environment as well as the integrity of the film formed indicated by different steady state potentials

| Electrolyte | $R_s$ ($\Omega$ cm$^2$) | $R_{out}$ ($\Omega$ cm$^2$) | $CPE_{out}$ ($\mu$F/cm$^2$) | $n_{out}$ | W (mMhos$^{1/2}$) |
|---|---|---|---|---|---|
| Saline | 16.4 | 110 | 14.1 | 0.80 | 12.8 |
| PBS | 14.8 | 213 | 13.5 | 0.83 | 10.9 |
| PBS + 0.5gl$^{-1}$ BSA | 17.4 | 298 | 10.2 | 0.82 | 10.1 |
| PBS + 2.0gl$^{-1}$ BSA | 18.1 | 321 | 8.4 | 0.80 | 8.9 |
| PBS + 4.0gl$^{-1}$ BSA | 19.3 | 342 | 5.8 | 0.83 | 7.38 |
| Saline + 4.0gl$^{-1}$ BSA | 16.8 | 227 | 9.2 | 0.80 | 11.1 |

**TABLE 5:** *The extracted values obtained from the electrochemical fitted circuit for cathodic conditions*

The curve obtained after the potential is shifted from cathodic to passive can be fitted to a second order decay curve to determine the kinetics of repassivation. The second order fit applied to the alloy in PBS is indicated in Figure 11. This second order model accounts for both the coverage and thickening phases of film formation. Firstly it describes lateral growth of the film to cover the surface of the alloy and also increasing thickness of the film until fully developed. From the graph it is observed that the coverage phase ($\tau_1$) is dominant as this is where the current falls drastically from peak current towards the passivation current. After that the current descends at a much slower rate towards passivation which is indicative of the thickening phase ($\tau_2$).

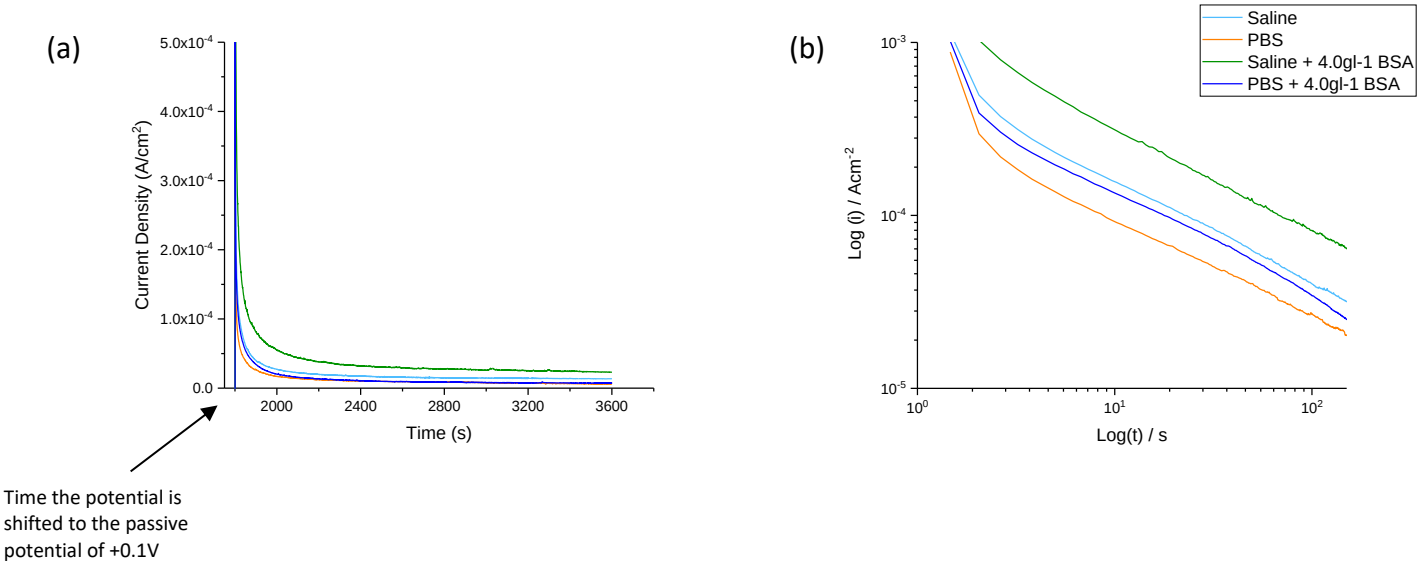


**FIGURE 10:** *The rates of repassivation for CoCrMo in simulated biological environments*

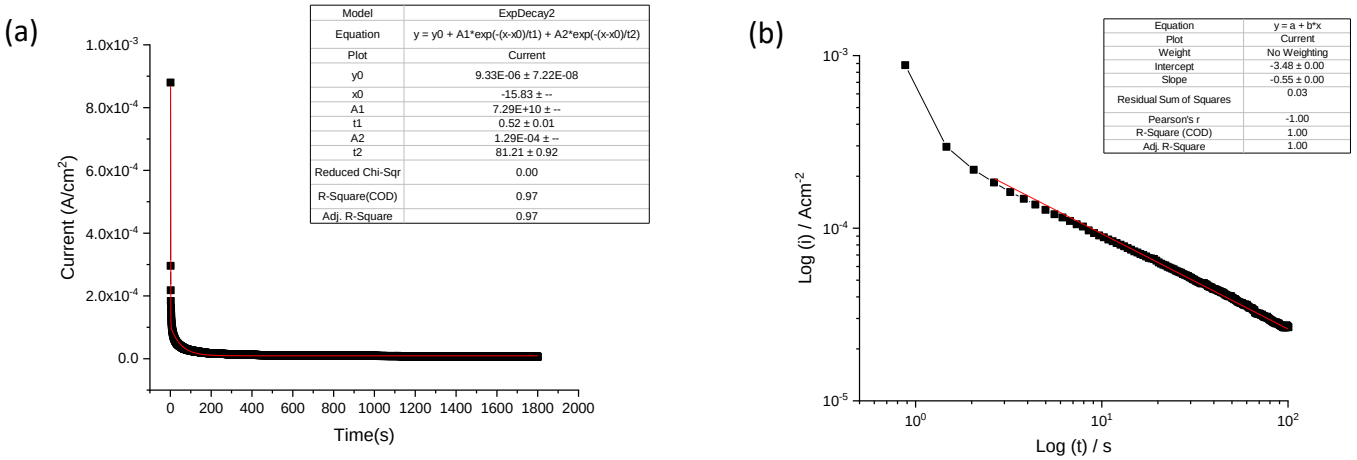


**FIGURE 11:** *Example of the 2nd order exponential fit (a) and determination of repassivation index (b)*

Figure 12 shows the values of the exponential fits for $\tau_1$ and $\tau_2$. Repassivation occurs fastest in a PBS environment, with BSA delaying this process as the protein inhibits the oxygen reduction reaction by blocking the active sites of the metal when adsorbed onto the surface of the alloy.

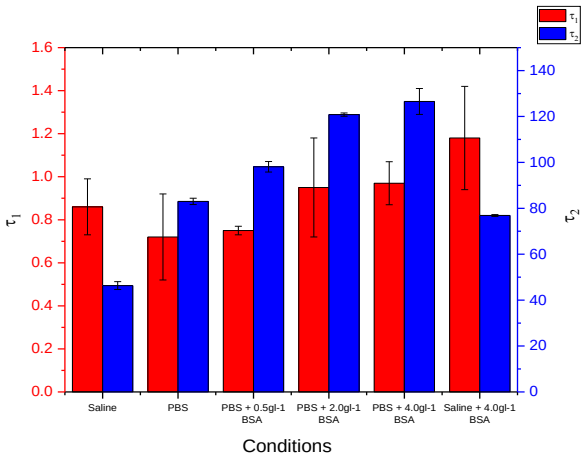


**FIGURE 12:** *Comparison of the obtained time constants determined from the repassivation data of CoCrMo*

The integrity of the film formed on the surface of the metal was determined from the current transients by plotting them on a Log-Log scale which allows the repassivation index to be obtained via analysis of the slope as explained previously. Figure 6 shows the current transients on a Log-Log scale, with the extracted repassivation index values being shown in Table 6.

| Electrolyte Used | Repassivation Index |
|---|---|
| Saline | -0.41 ± 0.01 |
| PBS | -0.52 ± 0.02 |
| PBS + 0.5gl$^{-1}$ BSA | -0.50 ± 0.01 |
| PBS + 2.0gl$^{-1}$ BSA | -0.46 ± 0.02 |
| PBS + 4.0gl$^{-1}$ BSA | -0.44 ± 0.02 |
| Saline + 4.0gl$^{-1}$ BSA | -0.39 ± 0.01 |

**TABLE 6:** *Repassivation Index values obtained for a variety of simulated bodily fluids*

From the data obtained in Table 6 it is shown that the film formed in PBS is the most protective, with the presence of BSA slowly weakening the film and increasing the porosity of the film which is due to competitive binding with the oxidant to the surface of the alloy. As expected the weakest film is seen in the absence of PBS with albumin.

## *XPS Analysis*

After the electrochemical tests, the surface of the alloy was examined via XPS to investigate changes in the passive film composition. Analysis of the alloy signaled the presence of these following elements: carbon (C 1s), oxygen (O 1s), chromium (Cr 2p), cobalt (Co 2p), molybdenum (Mo 3d). In the PBS environments, phosphorus (P 2p) was also detected with nitrogen (N 1s) and traces of sulfur (S 2p) being observed when BSA was present.The deconvoluted peaks for the species of interest are depicted in Figure 13.

PBS Environment

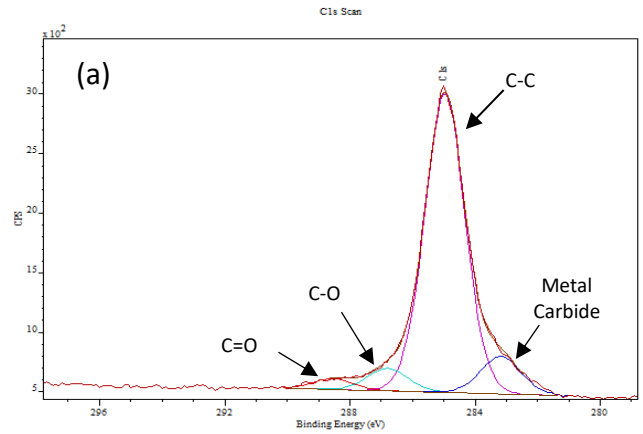


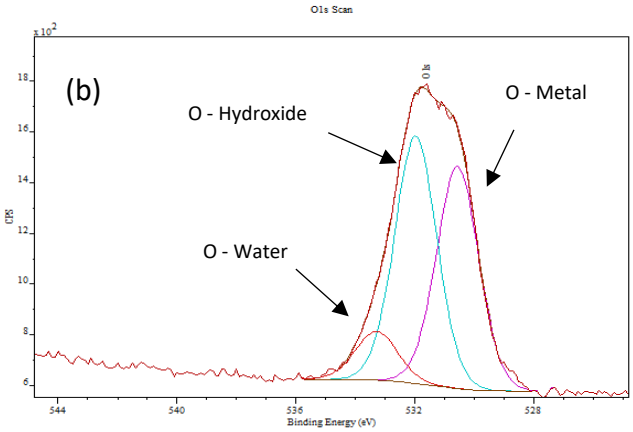


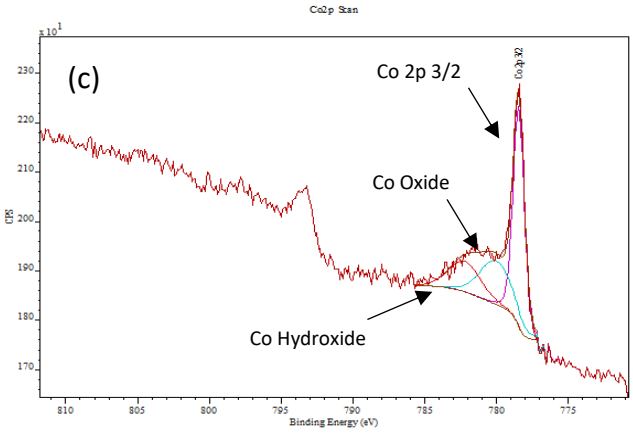


PBS + 4.0gl$^{-1}$ Environment

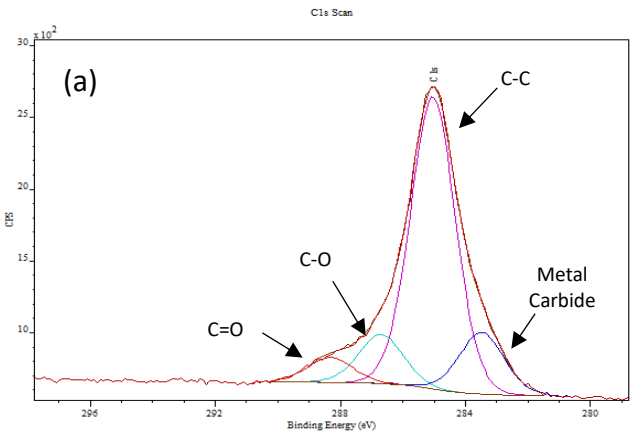


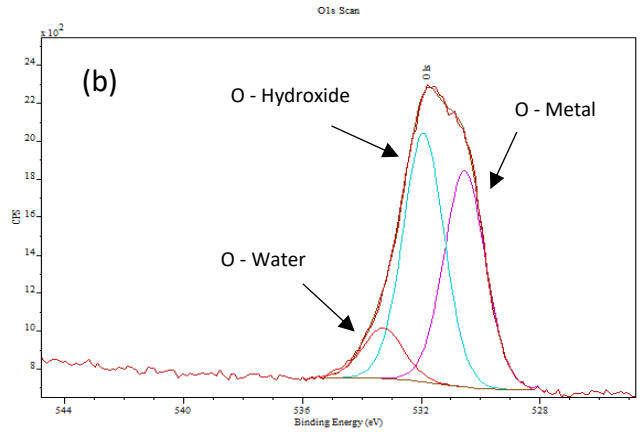


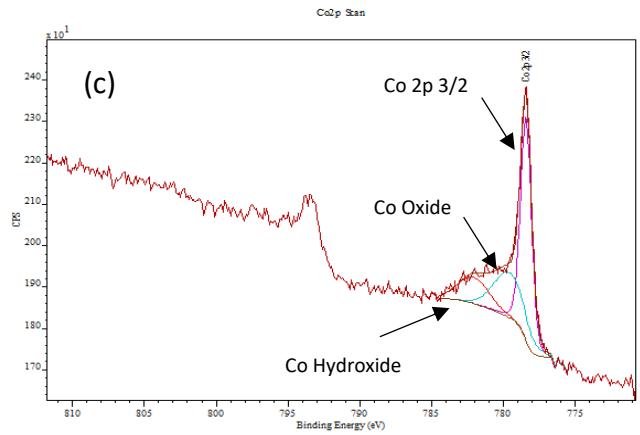

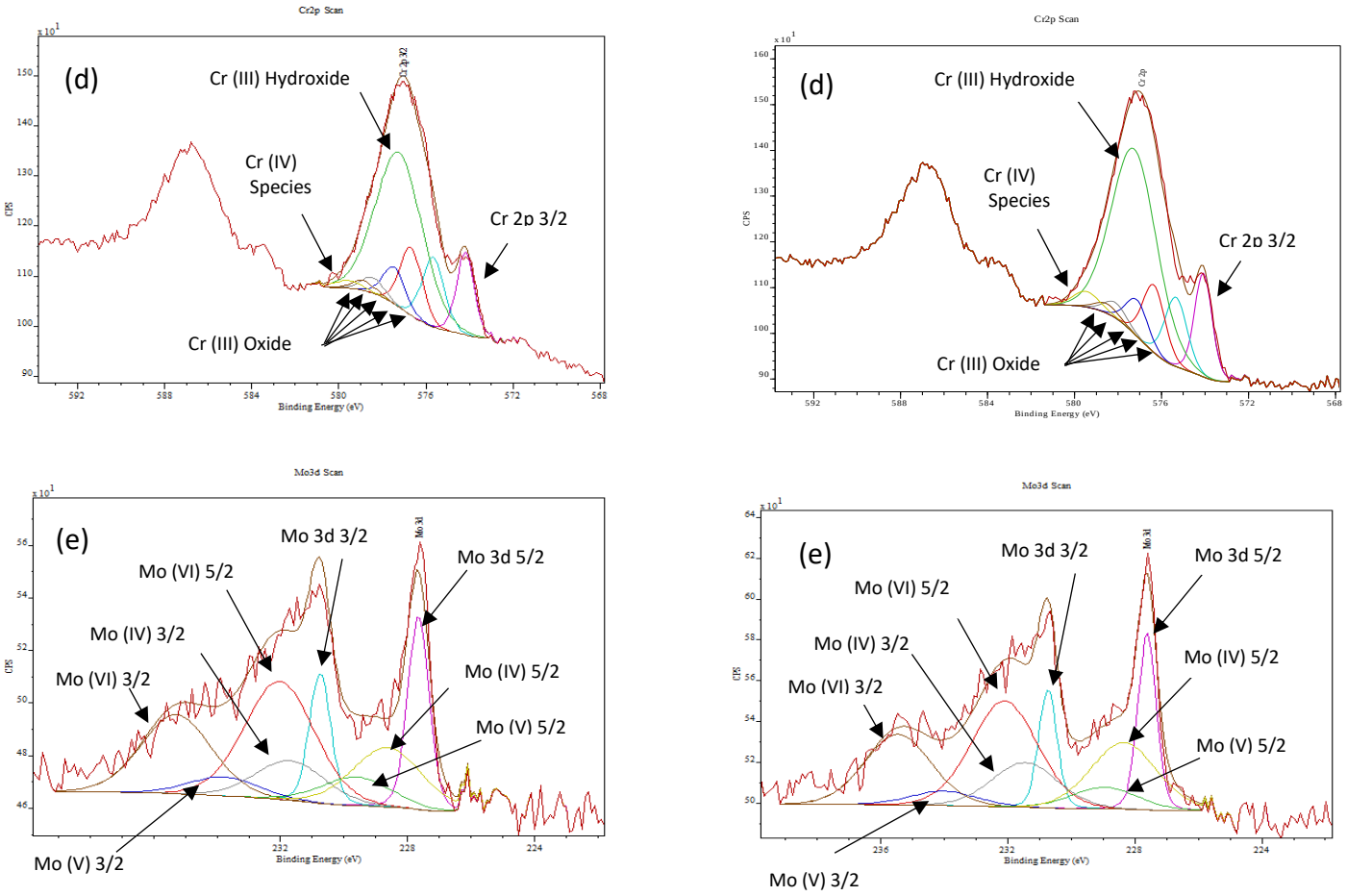


**FIGURE 13:** *Fitting of XPS peaks on the repassivated surface for CoCrMo alloy in PBS and PBS with 4.0gl$^{-1}$ BSA: (a) Carbon, (b) Oxygen, (c) Cobalt, (d) Chromium and (e) Molybdenum*

The presence of BSA causes alterations in the C 1s spectra of the alloy shown in Figure 9b, with a higher percentage carbon existing as either C-O or C=O. There is a broadening of the peak which indicates that BSA is adsorbed on the surface. This can be backed up by the emergence of N 1s peak that is seen alongside the presence of albumin, this peak is shown in Figure 14.

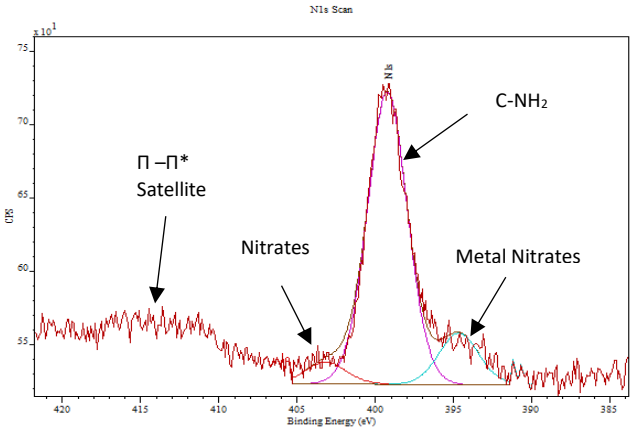


**FIGURE 14:** *Nitrogen (N 1s) XPS peak of the repassivated sample in PBS + 4.0gl$^{-1}$ BSA*

The metal peaks are defined by a sharp peak with the degree of oxidation increasing the binding energy slightly. Co is observed to mainly exist in its metal form for both conditions with a slight increases in hydroxide being formed in the presence of albumin shown in Figure 13c. The chromium exists primarily as Cr(III) oxide and hydroxide, with the ratio of both $Cr_{metal/oxide}$ and $Cr_{metal/hydroxide}$ increasing in the presence of protien indicated in Figure 13d. There are many different peaks of Cr(III) oxide due to multi split components.[21] In Figure 13e the molybdenum peaks are shown, for all conditions the +6 oxidation state of molybdenum is highly favored with percentage increases in the +4 state when exposed to albumin which could be attributed to bound molybdenum to the protein on the surface of the alloy.

The percentage of metallic elements Co, Cr and Mo within the passive film of the alloy is shown in Figure 15, determined via deconvoluting the individual spectra and calculating the quantity of the metal present in the oxide state. This obtained data can help understand the composition of the film under different environments.

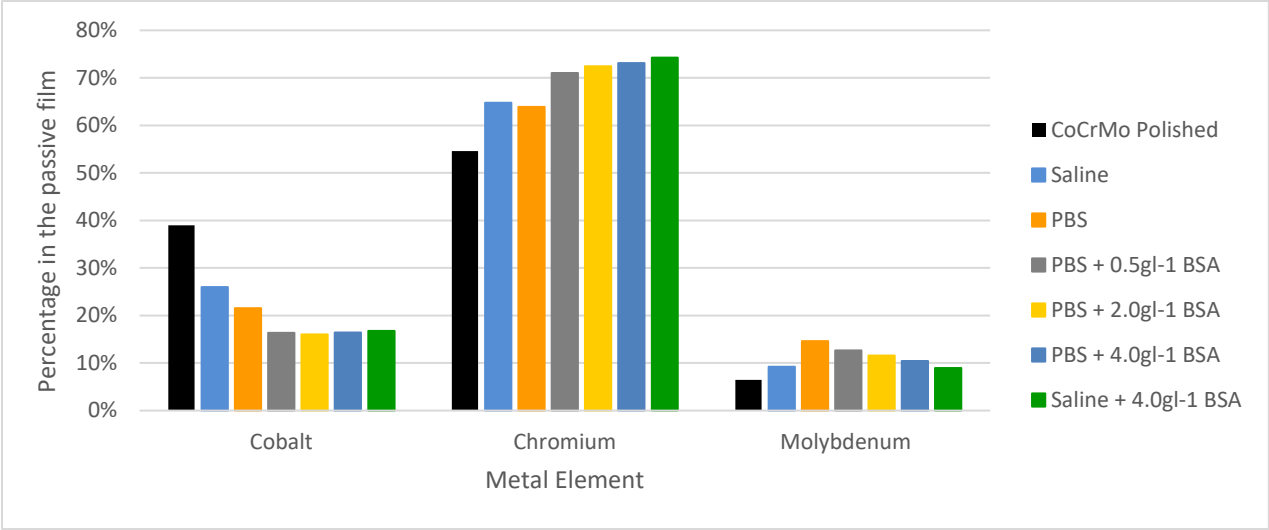


**FIGURE 15:** *Percentage of metallic elements present in the oxide state under a range of biological conditions*

From the data in Figure 15 it can be seen that passive film formation is effected quite drastically by its surrounding environment altering the metal ion contributions within the film. The main constituent of CoCrMo is Cobalt (~66%), when the oxide layer is produced in saline the content of cobalt within the film is highly diminished in comparison to an air formed film and even more so when exposed to phosphates and albumin. Chromium has the highest presence within the passive film due to it having the lowest standard reduction potential out of the metals present and is therefore the most favorable metal to be oxidized. The content of molybdenum within the oxide layer increases in PBS but as albumin is added it actually decreases, this is due to the high affinity between this metal ion and the albumin which causes molybdenum to be extracted into the bulk solution thus lowering its concentration in the film.

## *ICP-MS Analysis*

The content of metal dissolution from the alloy in µg/L in shown in Figure 16. In saline conditions, the majority of ions released are cobalt which exceeds the stoichiometry in the alloy.

This is attributed to the fact that cobalt forms dissolved ions whereas chromium ions form a solid oxide. The effect of phosphates causes an increase in chromium ions at the expense of cobalt owed to chromium being drawn towards the surface due to the environment, being in more agreement with the stoichiometry of the alloy. When Albumin is added, the release of molybdenum ion drastically increases due to the high affinity with the protein molecule which is in agreement with the XPS work carried out.

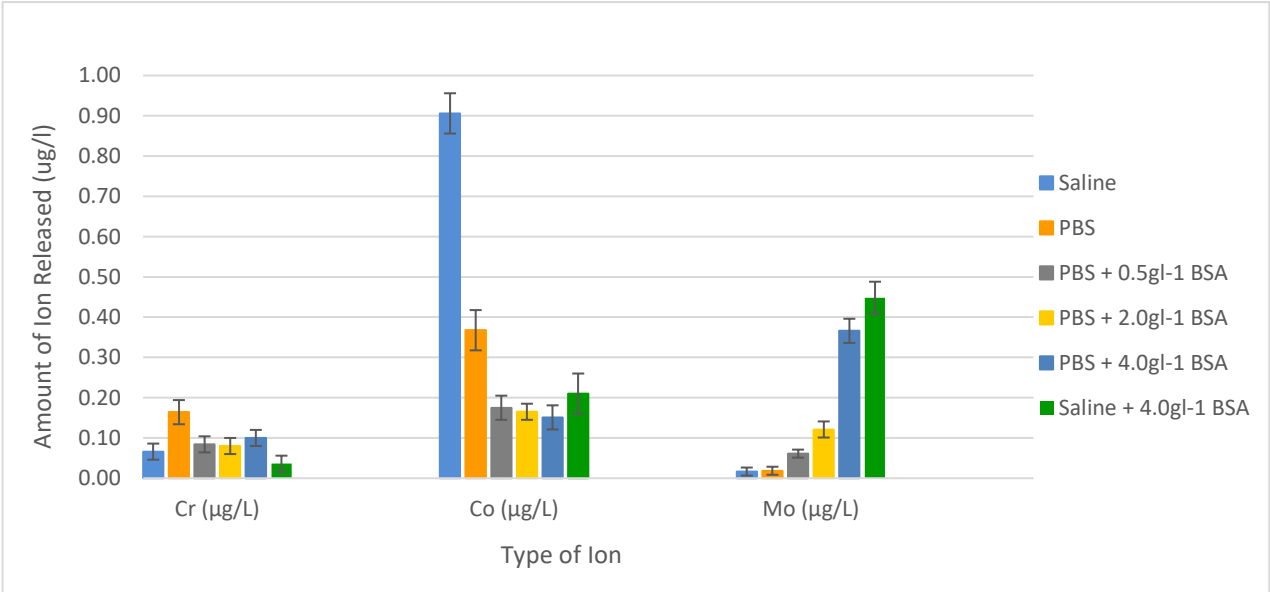


**FIGURE 16:** *Amount of metal ions released from the alloy into the bulk solution*

### *Charge Density*

By using Faraday's Law, depicted in Equation 7 it was possible to convert the quantities of metallic ions detected into the total charge lost. The total charge for each of the metal ions under a specific conditions is depicted in Figure 17, with a comparison against the total charge density determined from the integration of the current transients shown in Table 5.

$$Q = \frac{mFz}{M}$$

**EQUATION 7:** *Faraday's Law of Electrolysis*

Where: m = mass of the substance liberated at an electrode in grams, F = the faraday constant, M is the molar mass of the substance in grams/mol and z is the valancey number of ions of the substrate. (Co = 2, Cr = 3, Mo = 4)

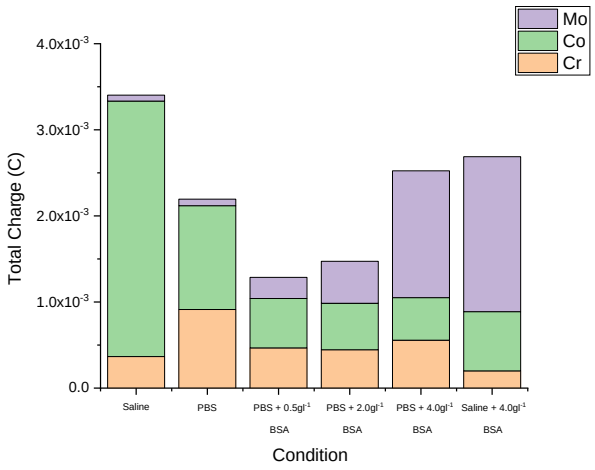


**FIGURE 17:** *The charge of ions released into the bulk solution determined by Faradays Law ($Q_{Diss}$)*

| Condition | $Q_{Diss}$ (mC) | $Q_T$ (mC) |
|---|---|---|
| Saline | 3.40 ± 0.32 | 2.18 ± 0.15 |
| PBS | 2.19 ± 0.37 | 1.15 ± 0.09 |
| PBS + 0.5gl$^{-1}$ BSA | 1.29 ± 0.25 | 1.22 ± 0.16 |
| PBS + 2.0gl$^{-1}$ BSA | 1.47 ± 0.26 | 1.53 ± 0.11 |
| PBS + 4.0gl$^{-1}$ BSA | 2.52 ± 0.33 | 2.09 ± 0.13 |
| Saline + 4.0gl$^{-1}$ BSA | 2.85 ± 0.29 | 3.02 ± 0.22 |

**TABLE 7:** *A comparison between the charge of dissolution measured by ICP-MS ($Q_{Diss}$) and the total charge ($Q_T$) determined by integration of the current transients obtained*

From the data extracted it is seen that the charge of dissolution decreases in the presence on phosphates due to sufficient decreases in charge contributions from both cobalt and chromium ions, with little effect seen on molybdenum. When BSA is part of the environment the quantity of charge owed to molybdenum increases as the concentration of BSA does attributing to over half of the overall charge when present at 4.0gl$^{-1}$ in solution. In terms of overall charge, the $Q_{Diss}$ accounts for the vast majority of total charge for all environments.

## DISSCUSSION

The corrosion resistance of CoCrMo is related to the formation of a passive film on the surface of the alloy which acts as a barrier to the environment, limiting corrosion. Once stripped of this film its ability to repassivate at a high rate is key to prevent metal ions being released into the body. It is well known that an alloy with a higher rate of repassivation possesses a higher corrosion resistance as less corrosion occurs per repassivation phase. The results obtained document that the presence of BSA reduces the rate of repassivation, alters the composition of the newly formed film and the rate of metal ion release. It has been seen in other literature that BSA can have beneficial effects on the corrosion behavior, seen in work from Y.Yan,[8] where albumin formed a biofilm which reduced metal ion release. From the work carried out, this would only be true when the surface is in a passive state but has adverse effects if the passive film is compromised.

The corrosion behavior of the alloy under both passive and cathodic was investigated by use of EIS. Under these conditions the presence of phosphates increases the corrosion resistance of the alloy indicated by increased values of $R_p$ which is in good agreement with the potentiostatic and potentiodynamic data obtained as a phosphate environment gave the lowest values of $i_p$. The presence of BSA increases the values of $R_{out}$ and $CPE_{out}$ for both conditions which implies that the molecules absorb onto the surface protecting the alloy from the environment.
The impedance under passive conditions consist of high values of $10^5$ which is characteristic of a passive film for a CoCrMo alloy. The equivalent circuit used to model this data has been used by multiple authors to when modelling the passive state of CoCrMo.[22,23,24] Whereas the impedance values for cathodic conditions are highly diminished alongside with a greater capacitance indicating that the passive film has vastly been reduced due to the cathodic reaction being favored.[25] The circuit fitted for the impedance spectra under cathodic conditions has a warburg component due to the line at high frequencies off the small semicircle, this has been modeled in this way previously by C.Vidal.[24] They stated that this frequency loop represents the diffusion of dissolved oxygen.
From undertaking EIS under both of these conditions it can be said that the oxide film under these cathodic conditions has majorly/fully been reduced. This is in concordance with findings in the literature in that little/no oxide forms if the potential becomes sufficiently negative (less than -0.5V vs Ag/AgCl) .[22,25,26]

The kinetics of repassivation was studied by analyzing the time constants obtained from the current transients. From the data shown in Figure 7, the presence on BSA delays the rate of repassivation by hindering both the coverage and thickening phases of the passive film. Due to BSA adsorbing onto the surface impeding access of dissolved oxygen to the metal surface.[27,28] Work by D.Sun,[29] also saw a greater repassivation time in a protienous environment when the film was compromised via a scratch test and suggested the gradual re-establishment of the electric double layer contributes to the slow recovery of current. These theories are backed up from the data obtained from the polarization data of CoCrMo where the protein was shown to act as a cathodic inhibitor. As $\tau_1$ is shown to be the dominant time constant, a longer $\tau_1$ causes the alloy to undergo more corrosion as the time for the alloy to be covered by the protective oxide film increases thus increasing the quantity of metal ions released. In the presence of BSA, there is more time for the molybdenum ions to be extracted into the bulk solution. This effect is further amplified in the absence of phosphates as its well known that phosphates compete to bind to the surface of the alloy with BSA and as the phosphate ion is an

oxidizing agent it helps contribute the reformation of the passive film.[7,30] By looking at the values of $\tau_2$ it is seen that the thickening of the oxide film occurs quickest in the absence of PBS, with presence of BSA also slowing down this rate. This is down to the oxidant needing to diffuse through the adsorbed BSA layer on the surface as well as the newly formed oxide film to reach the surface of the alloy and be reduced, this causes a slow growth of the film to its maximum state. As expected the obtained steady state current was lowest in a PBS environment as the phosphates adsorbs onto the surface protecting the alloy thus lowering the current density**.** With the thickening of the film also being inhibited in an albumin environment as well as the overall porosity of the film this could lead to an increase in dissolution of metal ions if they can diffuse away through the newly covered alloy. There have been reports of repassivation occurring on the millisecond time scale when the oxide film has been removed via scratch testing as seen by J.R Goldberg and D.Sun.[13,29] This can be attributed to the extent and complexity of the area in question with this study being on a much greater scale compared to a single scratch. Upon mechanical depassivation, deformation of the area occurs which may alter the corrosion potential of the surface leading to a faster rate of repassivation.[31] This also leaves oxide present either side of the depassivated area enabling passivation to occur via lateral growth which isn't present in this case.

Alongside the passive film being reformed at a reduced rate, the composition of the film formed after repassivation is also altered drastically depending on the condition. Li et al,[32] saw alterations in the passive film composition under wear-induced conditions, seeing the percentage of chromium with the film after repassivation decreasing. As expected, the reformed passive film mainly consists of chromium (III) oxide and chromium (III) hydroxide which is characteristic of CoCrMo alloys.[30,33,34] In the presence of albumin the content of cobalt is diminished to ~17%, Milosev and Strenblow,[33] determined that the concentration is typically 25% in a passive layer, which is quite an increase on that of a reformed oxide. The presence of molybdenum is reduced with increasing quantities of albumin in the environment, this is contradicting to work carried out on passivated samples. Munoz and Mischler,[30] documented that in the presence of albumin the presence of molybdenum increases within the film when a CoCrMo sample is passivated under electrochemical conditions.

By taking into account that the reformed film is consists primarily of chromium (III) oxide film to be off a thickness of 2nm with a density of 5.22gcm$^{-3}$ due to repassivation occurring under a passive potential, the charge of film formation is 0.75mC for the area of the sample in question.[9] For several of the environments it is seen that the charge of dissolution is greater than the total charge determined experimentally. This calculated total charge density is an underestimation of the true value as it doesn't take into account the iR drop alongside some limiting factors which are discussed later on. By comparing the charge needed for film formation to the charge of dissolution it is clear that the majority of the total charge is attributed to the dissolution of metallic ions which is well supported by the literature.[9,35] This is further supported by the data in table 7 which presents a close agreement between $Q_{Diss}$ and $Q_T$ with respect to experimental error. The charge of dissolution as well as the total charge is highly diminished when phosphates are present due to quicker reformation of the oxide film, with the ratio of the charge of ions released stays relatively constant. Albumin causes a drastic increase in the total charge due to the higher rates of repassivation alongside the reduction of BSA molecules enabling them to adsorb onto the surface. The ratios of charge owed to dissolution is shifted to favor molybdenum ions indicting that the albumin extracts the ion into the bulk, this electrochemical interactions between these could also contribute to the increased total charge observed.

The comparison of molybdenum content for passivated and repassivated samples is intriguing as, from Munoz and Misclers work it was observed that the percentage of molybdenum in the film increased up to ~14% when in the presence of albumin in both saline and PBS conditions.[30] From the data shown in Figure 11 ,the percentage of molybdenum decreases under repassivation to ~9% and ~10% in the presence of albumin in saline and PBS respectively. There is a decrease in molybdenum content when the passive film is compromised in the presence of molybdenum as the metal ions have a high affinity for the protein allowing them to diffuse away into the solution, this is not possible when the film is present, this process is shown in Figure 18. The presence of molybdenum seems to play a vital role in the integrity of the oxide film formed with porosity of the film increasing as the presence of molybdenum in the film is reduced as seen in Table 6. This can be deduced as the presence of chromium increases which is well known to increase corrosion resistance.[10,15,27] The decreasing values of OCP and rising $i_p$ in BSA solutions from the potentiodynamic experiment back this up as they indicate that the passive film is less protective. The differences in the passivated and repassivated films alongside the EIS data obtained are also another reason to support that the conditions to reduce the air formed oxide were successful.

From analyzing the solutions after each electrochemical experiments it is shown that BSA can complex to metal ions and extract them into solution, specifically molybdenum which accelerates the dissolution process of the alloy,[28,34] This mechanism helps explain the observed increase in $i_{corr}$ with albumin containing solutions obtained from the potentiodynamic experiments in Figure 5a. The preferential binding of the molybdenum ion to the protein has also been documented in the literature several times.[9,36,37] In the electrolyte the overall globular charge of the protein molecule is negative as the carboxylate groups become deprotonated due to the isoelectric point of BSA being 4.7. [6,7,10] It is these negative functional groups that can bind with the positive metal cations via electrostatic interactions forming an irreversible bond.[10,37] The formation of covalent bonds and wettability are significant in binding of metal ions to the active sites in BSA.[6] A possible interaction that could take place is the binding of the molybdenum cation to the free sulphur group on cysteine-34 which is known to be a very thermodynamically favored bond, this could explain why molybdenum binds preferentially over the other two metal ions present. This in turn causes the composition of the passive film to be altered after repassivation which effects the integrity of the film and future performance of the implanted alloy.

By looking at how the bare metal surface interacts with a protein environment compared to that of an alloy protected by a passive film it is possible to deduce that the passive film protects the alloy from interactions with the protein.[38] The protein molecules are seen to have weak and reversible interactions with the oxide film as it's a relatively unreactive, apolar surface consisting of chromium oxide.[10,38] When the oxide film is cleaved the reactive surface is exposed causing electronic interactions to be more pronounced which leads to stronger interactions and dissolution of the metal ions as shown in Figure 18.

## LIMITATIONS

The potentiostatic methods utilized within this research are desirable in predicting the behavior of alloys under different conditions, but there are multiple factors which can influence/effect the obtained data ranging from the response time of the equipment used to the rate of oxide removal.[35]

Limitations with this specific data set obtained are due to ohmic limitations as well as the response time of the potentiostat which fails to collect data on the nanosecond scale.[35,39] As the response time of the potentiostat is low it means that a portion of charge is lost in the early stages as it cannot increase the current at a fast enough rate to maintain the potential which is needed due to the rapid change from cathodic to passive potentials.[35] The vast change in the conditions also leads to an ohmic drop which causes an effect on the early portion of the current transient formed.[35,39] Due to these limitations the data set is only instructive with respect to the trend of solution analysis.

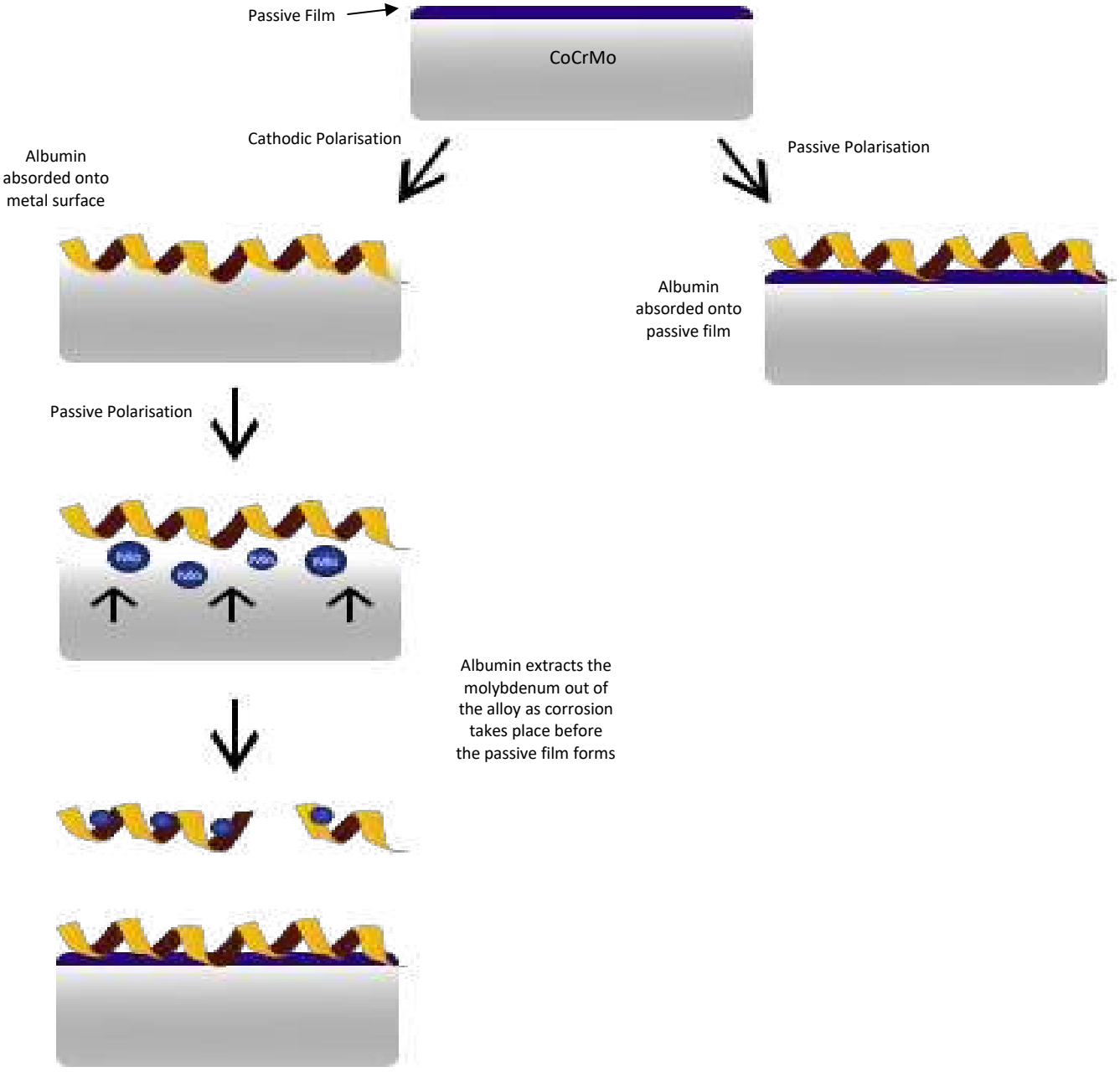


**FIGURE 18:** *Schematic showing the process of molybdenum extraction in the presence of BSA when electrochemical repassivation is undertaken against passive polarization*

## *Conclusion*

An in depth analysis was undertaken on the kinetics and composition of an electrochemically repassivated oxide CoCrMo film in a variety is simulated bodily fluids, from the results obtained the following conclusions have been reached:

1. The environment in which repassivation occurs has a drastic effect on the rate of repassivation with the quickest occurring in a phosphate containing environment whilst if BSA is added the rate slowly decreases as oxidant is inhibited due to the size of the protein which blocks the active sites of the alloy
2. Presence of Albumin causes the passive film to become less compact and therefore increase in porosity
3. The composition of the passive film is drastically altered when albumin is added, reducing the quantity of molybdenum by extracting the metal element into the bulk solution. This could lead to the integrity of the film being compromised after prolonged periods of time
4. With the presence of albumin in the electrolyte, there is a drastic increase in molybdenum released from the alloy due to high binding affinites

# REFERENCES


1. V. Sansone, D. Pagani, M. Melato,"The effects on bone cells of metal ions released from orthopedic implants.A review," Clinical Cases in Mineral and Bone Metabolism, 2013; 10(1): 34-40
2. R. Ferguson, A. Palmer, A. Taylor, M. Porter, H. Malchau, S. Jones," Hip Replacement," Lancet, 108, 392: 1662-71
3. Y. Liao, E. Hoffman, M. Wimmer, A. Fischer, J. Jacobs, L. Marks,"CoCrMo metal-on-metal hip replacements," Phys.Chem.Chem.Phy.,2013, 15, 746
4. S.R. Knight, R. Aujla, S.P. Biswas," Total Hip Arthroplasty – over 100 years of operative history," Orthopedic Reviews. 2011; 3(2): e16
5. A.G. Cobb, T.P. Schmalzreid," The clinical significance of metal ion release from cobalt-chromium metal-on-metal hip joint arthroplasty", J. Engineering in Medicine, 2006, 220(Part H)
6. C. V. Vidal, A. I Munoz, C.A. Olsson, S. Mischler, "Adsorption of BSA on Passivated CoCrMo PVD Alloy: An EQCM and XPS Investigation," J. The Electrochemical Society, 2014, C294-C301
7. C.V. Vidal, A.O. Juan, A.I. Munoz, " Adsorption of bovine serum albumin on CoCrMo surface: Effect of temperature and protein concentration," Colloids and Surfaces B: Biointerfaces, 2010, 1-11
8. Y. Yan, A. Neville, D. Dowson, "Biotribocorrosion of CoCrMo orthopaedic implant materials – Assessing the formation and effect of the biofilm," Tribology International, 2007, 40,1492-1499
9. N. Espallargas, C. Torres, A.I. Munoz, "A metal ion release study of CoCrMo exposed to corrosion and tribocorrosion conditions in simulated body fluids," Wear 332-333. 2015; 669-678
10. R.L. Williams, D.F. Williams," Albumin adsorption on metal surfaces," Biomaterials, 1998, 9, 206-212
11. J. Ambrose," Repassivation Kinetics," Treatise on Materials Science and Technology, Vol 23, 1983, p 175-204
12. J.Gilbert," Electrochemical Behavior of Metals in the Biological Milieu," Comprehensive Biomaterials II, Ch 1.2, 2017
13. J.R. Goldberg, J.L Gilbert," Electrochemical response of CoCrMo to high speed fracture of its metal oxide using an electrochemical scratch test method", Division of Biological Materials and Department of Biomedical Engineering, 1997, 27(3), 421-431
14. D.Sun, J.A Wharton, R.J.K Wood," Abrasive size and concentration effects on the tribo-corrosion of cast CoCrMo alloy in simulated body fluids," Tribology International, 2009, 42, 1595-1604
15. J. Lee," Effects of alloying elements, Cr, Mo and N on repassivation characteristics of stainless steels using the abrading electrode technique," Materials Chemistry and Physics, 2006, 99(2-3), pp.224-234
16. M.Bryant, A.Neville," Corrosion and Mechanical Properties," Orthopedics and Trauma, 2016, 30, 176-191
17. D. Jones, N. Greene,"Electrochemical Measurement of Low Corrosion Rates," Corrosion, 22(7), 198-205, 1966
18. G.Berry, J. Bolton, J. Brown, S. McQuaide, "The Prodcution and Properties of Wrought High Carbon Co-Cr-Mo Alloys," Cobalt-Base Alloys for Biomedical Applications, ASTM STP 1365, 1999
19. S. Mahiya, G.Lofrano, S.K. Sharma, " Heavy metals in water, their adverse health effects and Biosorptive removal: A review," International Journal of Chemistry, 2014, 3(1), 132-149
20. A.V Naumkin, A. Kraut-Vass, S.W Gaarenstroom, C.J Powell, " NIST X-ray Photoelectron Spectroscopy Database," NIST Standard Reference Database 20, Version 4.1
21. M.C. Biesinger, B.P Payne, " Resolving surface chemical states in XPS analysis of first row transition metals, oxides and hydroxides: Cr, Mn, Fe, Co and Ni," Applied Surface Science, 2011, 257, 2717-2730
22. A.Munoz, C.Vidal," Influence of electrochemical conditions on CoCrMo behaviour in simulated body fluid by step polarization technique," ECS Transactions, 2010, 28(24), 23-25
23. J.Cassar, B. Mallia, A. Karl, J. Buhagiar," EIS of carburized CoCrMo: Evolution of parameters characterizing the metal-electrolyte interface," Surface and Coatings Technology, 2016, 292, 90-98
24. C.Vidal, A.Munoz," Electrochemcial Aspects in Biomedical Alloy Characterization: Electrochemical Impedance Spectrosopy," Biomedical Engineering: Trends in Materials Science, 2011, 283-306
25. M. Haeri, S. Goldberg, J.L.Gilbert," The voltage-dependanet electrochemical impedance spectroscopy of CoCrMo medical alloy using time-domain techniques:Generalized Cauchy – Lorentz, and KWW-Randles functions describing non-ideal interfacial behaviour," Corrosion Science, 2011, 53, 582-588
26. V.Swaminathan, J.L Gilbert, "Potential and frequency effects on fretting corrosion of Ti6Al4V and CoCrMo surfaces," J. Biomedical Materials, 2013, 101(9), p2602-2612
27. S. Virtanen, I. Milosev, E. Gomez-Barrena, R. Trebse, J. Salo, Y.T Konttinen, "Special modes of corrosion under physiological and simulated physiological conditions," Acta biometerialia, 2008, 4, 468-476
28. X. Cheng. S. G. Roscoe," Corrosion behavior of titanium in the presence of calcium phosphate and serum proteins," Biomaterials, 2006, 25, 7350-7356
29. D.Sun, J.A Wharton, R.J.K Wood," Micro- and Nano-scale Tribo-Corrosion of Cast CoCrMo," Tribol Lett, 2011,41, p525-533
30. A.I. Munoz, S. Mischler," Interactive Effects of Albumin and Phosphate Ions on the Corrosion of CoCrMo Implant Alloy," Journal of The Electrochemical Society. 2013; 154(10), C562-C570
31. W.Li, D.Y.Li," Variations of work function and corrosion behaviors of deformed copper surfaces," Applied Surface Science, 2005, 240 (4), 388-395
32. X. Li, Y. Yan, H. Zhang, Y.Su, L. Qiao, " Depassivation- repassivation Behaviour of a CoCrMo Alloy under Tribological Contact in Simulated Body Fluids," Int.J.Electrochem.Sci, 2017, 2495-2505
33. I. Milosev, H.H Strehblow, "The composition of the surface passive film formed on CoCrMo alloy in simulated physiological solution", Electrochimica Acta, 2003, 48(19), 2767-2774
34. A.W.E. Hodgson, S. Kurz, S. Virtanen, V. Fervel, C. O.A. Olsson, S. Mischler," Passive and transpassive behaviour of CoCrMo in simulated biological solutions," Electrochim. Acta. 2004, 2167-2178

35. D.G Kolman, J.R Scully," Limitations of Potentiostatic Repassivation Techniques and their Relationship to the Applicability of the High Field Approximation to the Repassivation of Titanium", Journal of the Electrochemical Society, 1995, 142(7), 2179-2188
36. T.A. Simones, A.P. Brown, S.J. Milne, R.M.D Bryson," Bovine Serum Albumin binding to CoCrMo nanoparticles and the influence on dissolution," Journal of Physics, 2015, 644
37. T.A. Simones, M.G. Bryant, A. P. Brown, S.J. Milne, M. Ryan, A. Neville," Evidence for the dissolution of molybdenum during the tribocorrosion of CoCrMo hip implants in the presence of serum protein," Acta Biomaterialia, 2016, 45, 410-418
38. V. Maskiewicz, P. Williams, S. Prates, J. Bowsher, I. Clarke," Characterization of protein degradation in serum-based lubricants during simulation wear testing of metal-on-metal hip prosthesis," J. Biomed Mater Res Part B: Appl Biomater, 2010, 94(2), 429-40
39. G.T Burnstien, A.J Davenport," The Current-Time Relationship during Anodic Oxide Film Growth under High Electric Field," J. Electrochem.Soc, 1989, 136(4), 936-941

# FIGURE CAPTIONS